MEDWIN PUBLISHERS
Committed to create value for Researchers

Nanomedicine & Nanotechnology Open Access
ISSN: 2574-187X

Molecular Sphere Radii of H_2O and D_2O to Achieve Rotational Brownian Motion

Osuga T*

Yokohama, Kanagawa, Japan

***Corresponding author:** Toshiaki Osuga, Yokohama, Kanagawa, Japan, Email: artisankoshik@yahoo.co.jp

Research Article

Volume 5 Issue 3

Received Date: June 18, 2020

Published Date: July 01, 2020

DOI: 10.23880/nnoa-16000186

Abstract

The sphere radii $^{H2O}a_w$ and $^{D2O}a_w$ of H_2O and D_2O performing rotational Brownian motion (RBM) in the liquid state were calculated to be $^{H2O}a_w$ =1.44±0.01 Å at 0°C and $^{D2O}a_w$ =1.45±0.01 Å at 10°C, respectively, by substituting the previously measured dielectric relaxation time τ_{rel} into the dielectric relaxation formula (DRF), where 0°C and 10°C are close to the maximum density temperatures of 3.98°C for H_2O and 11.6 °C for D_2O, respectively. The sphere radii $^{H2O}a_w{}^b$ and $^{D2O}a_w{}^b$ of H_2O and D_2O in the vapour state were calculated to be $^{H2O}a_w{}^b$ = 1.4445 Å and $^{D2O}a_w{}^b$ = 1.4532 Å of H_2O and D_2O, respectively, using the van der Waals b constant. The sphere radius performing RBM in the liquid state was found to be similar to that of a single molecule in the vapor state because $^{H2O}a_w$ and $^{D2O}a_w$ determined by τ_{rel} are close to $^{H2O}a_w{}^b$ and $^{D2O}a_w{}^b$ of H_2O and D_2O, respectively, which is supported by the specific heat showing a sufficient rotational freedom in the liquid state. The liquid density decreasing with temperature from 0 to 50°C can be used to determine the thermal expansion rate vol= 7.9×10-5/°C of the water sphere radius. The radius $^{H2O}a_w{}^S$ of H_2O (Stokes radius) performing the translational Brownian motion is calculated by substituting the diffusion coefficient into the Stokes-Einstein equation (SEE). The radius expansion rates of rot of $^{H2O}a_w$ and trans of $^{H2O}a_w{}^S$ were calculated to be 3.0×10-4/°C and 2.0×10-3/°C using the DRF and SEE, respectively. The DRF was found to yield better expansion rate than the SEE does in the water sphere radius evaluation because rot / vol is 4 while trans / vol is 23.

Keywords: Stokes Radius; Einstein–Smoluchowski Relation; Stokes-Einstein-Sutherland Equation; Langevin Equation; Van Der Waals Equation; Oseen Equation

Abbreviations: DRF: Dielectric Relaxation Formula; EPF: Electrophoretic Formula; TBM: Translational Brownian Motion; RBM: Rotational Brownian Motion; SEE: Stokes–Einstein Equation.

Introduction

When a sphere of radius a is immersed in a Newtonian viscous fluid such as water, and it performs a one-dimensional translational motion, the resistive drag required to maintain a steady velocity is described by Stokes' law, which is derived from the Navier–Stokes equation [1,2]. When an electric field E is applied to the solvent water containing solute molecules regarded as spheres, the equilibrium between the electric force and the resistive drag moves the solute molecule with steady electrophoretic velocity, which is called the electrophoretic formula (EPF) [3-5]. According to Walden's rule, the vep follows the distinct change in the viscosity with temperature. Thus, the Avogadro number average is employed to ensure that a Navier–Stokes equation using a viscosity determined on a macroscopic scale is applicable to electrophoresis performed at a molecular scale.

When the solute molecule regarded as a sphere is immersed in solvent water, the thermal agitation causes the molecular sphere to carry out random walks in translational and rotational directions, which are called translational Brownian motion (TBM) and rotational Brownian motion

(RBM), respectively [3,4,6-10]. The time averages of the cumulative random walks cause the squared values of the translational and rotational average displacements to be proportional to time. These proportional coefficients are called translational (D) and rotational (D_{rot}) diffusion coefficients, respectively. When the solute and solvent are similar, the D is called the self-diffusion coefficient D_{self}. When the molecular sphere performs a rotational motion, a force couple (torque) is required to maintain a stationary angular velocity [1,8-10]. The D and D_{rot} are derived from the equilibria between the thermal energy and resistive drag (Stokes' law), and that between the thermal energy and the force couple, which are called the Stokes–Einstein equation (SEE) and the dielectric relaxation formula (DRF), respectively. A molecular radius can be calculated using the SEE, DRF, or EPF; that calculated using the SEE is called a Stokes radius. The radius is very frequently estimated from D using the SEE because the D can be measured without application of alternating or direct electric field. Two inaccuracies with regard to the Stokes radius have been noted [11-13]. First, a molecular radius calculated using the SEE will be smaller than the van der Waals (electron cloud) radius; [14] Second, the temperature dependence of the Stokes radius is very high; thus, Walden's law does not hold for the SEE; this tendency is most distinct for lower molecular weight (MW) molecules such as water (H_2O) and heavy water (D_2O) molecules [11-13].

Studies of the restricted diffusion coefficients; $^{res}D_{self}$ of water and ^{res}D of solute in the restricted water solvent are in progress. The values of $^{res}D_{self}$ in the porous materials have been measured, where the void ratio and water content rate are measured by comparing D_{self} in free water and $^{res}D_{self}$ in restricted water [15]. The $^{res}D_{self}$ observation using magnetic resonance (MR) imaging is attempted because $^{res}D_{self}$ provides useful diagnostic information of activity and lesions in living tissues [16,17]. Although the value of D for solutes in water is determined by optical measurements (OMs) [3,11-18]. The exact D at the zero-concentration limit should be interpolated using data at higher concentrations because the OMs requires solute concentration over 0.1 mol/ℓ and interactions between solutes modify the values of D [3,19]. MR imaging can determine the exact D of CAs of ppm concentration without being affected by the concentration, because MR imaging achieves a sensitivity 100–1000 times higher than that of OMs, where CAs are compounds that bind to paramagnetic ions [20,21]. When the movement of the CA diffusing from the inside of the blood tube to the surrounding lesion tissue is measured by MRI, the ^{res}D of the CA in the tissue is exactly determined because the clinical dose of the CAs is 0.1～0.5 mmol/ℓ. The ^{res}D of the CA can be converted to the $^{res}D_{self}$ of water in the lesion tissue using the ratio among molecular sizes of the CA and water, and apparent pore size of the tissue [22]. Although the $^{res}D_{self}$ of water in tissues is determined only in the direction perpendicular to the MR imaging slice, the ^{res}D of the CA can be determined for any direction. Thus, the diagnosis based on the indirect observation of the $^{res}D_{self}$ of water converted from ^{res}D of the CA in MR imaging of living materials can improve the accuracy of the diagnosis based on the direct observation of $^{res}D_{self}$ of water in tissue.

The inaccurate temperature dependence in calculating the radius of the water molecule using the SEE will lead to the inaccuracy in evaluating material void structures having water content because the Stokes radius is the basic scale for measuring the void space of materials. The radii of H_2O and D_2O molecules can be determined by RBM that occurs simultaneously with the TBM using the DRF based on the previously conducted measurements of the dielectric relaxation time [23,24] and viscosity [25,26]. The radius of water molecules regarded as spheres in the vapour state can be calculated from the van der Waals b constant [25,27,28]. The thermal expansion of the space occupied by one liquid water molecule can be calculated using the density change with temperature [25]. This study, therefore, aims to compare the sphere radii and its temperature dependences of liquid water, calculated using the DRF van der Waals b constant, density, and SEE, in order to examine the inaccurate temperature dependence of the SEE.

Theory

A water sphere of radius and mass M is considered. The mass M of one water molecule is $M = 18m_p$, where m_p is the proton mass (1.67×10^{-27} kg). The distance between the hydrogen and oxygen nuclei r_{OH} is 0.9575 Å and the HOH angle θ_{HOH} is $\theta_{HOH} = 104.45°$. The x-y plane involving two hydrogen's and oxygen is shown in Figure 1(a), where the z-axis is vertically oriented. The Centre of gravity of the water molecule exists approximately at the Centre of the oxygen nucleus, and the two hydrogen atoms (protons) rotate around the oxygen nucleus. The three moments of inertia I_x, I_y, and I_z along the x, y, and z-rotation axes, are considered in Figure 1(b–d), respectively. Using these assumptions, $Iz = 2m_p r_{OH}^2$. The straight line connecting the two hydrogens is indicated by r_{HH} and the distance between the oxygen nucleus and the centre of r_{HH} is $r_{O\text{-}HH}$, where $r_{HH} = 1.51 + \left(\text{参} 2r_{OH} \bullet \sin(104.45°/2)\right)$ $r_{HH} = 2$ (=2 r_{OH} · sin(104.45°/2)) and $r_{O-HH} = 0.586 + \left(\text{参} r_{OH} \bullet \cos\left(104.45°/2\right)\right)$ $r_{O\text{-}HH}$= 0.586□ (= r_{OH} · cos(104.45°/2)). Thus, $I_x = 2m_p r_{O-HH^2}$ $I_x = 2m_p r_{O\text{-}HH}^2$ and $I_y = 2m_p \left(r_{HH}/2\right)^2$ $I_y = 2m_p (r_{HH}/2)^2$. The average $I\left[= \left(I_x + I_y + I_z\right)/3\right]$ I [= $(I_x + I_y + I_z)/3$] of I_x, I_y, and I_z

is assumed to be the moment of inertia for the water sphere rotation as

$$I = \frac{4}{3} m_p r_{oH}^2 \quad (2.1)$$

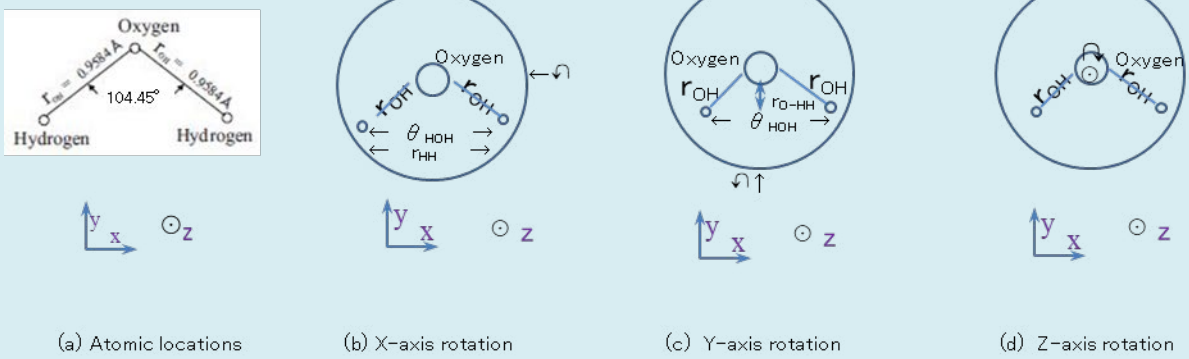

Figure 1(a): Locations of two hydrogen's and one oxygen in water molecule. Rotations of the water sphere (electron cloud) along (b) x-, (c) y-, and (d) z-axes around the rotation axes passing through the oxygen nuclei (centre of gravity).

Where the factor $4/3$ is derived from $\left(2+2\sin^2\left(104.45^\circ/2\right) + 2\cos^2\left(104.45^\circ/2\right)\right)/3$ $(2+2\sin^2(104.45°/2) + 2\cos^2(104.45°/2))/3$ as shown in Table 1.

Because the hydrogen and oxygen atoms are positively and negatively charged, respectively, the water molecule forms an electric dipole moment p_{H2O}. Because the dipole consists of one positive charge and one negative charge separated by a dipole length r_D, it is assumed that the positive charges of the two hydrogens are concentrated into single hydrogen and that r_D is equal to the distance r_{OH} between the hydrogen and oxygen nucleus. Fractional atomic charges of $q_O = -0.3990e$ and $q_H = +0.3990e$ are allocated to the oxygen and hydrogen nuclei, respectively, when constructing the dipole p_{H2O}, where e is the elementary charge (1.602×10−19 C). Thus, the dipole p_{H2O} is determined to be p_{H2O} = (0.3821 Å) e [10,29]. Although an electric field is applied on the dipole to artificially change the molecular rotation in the dielectric relaxation measurement, the electrically modified rotation is negligibly lower than the thermal rotation as shown in Section 3.

Rotation Axis	Formula	Moment of Inertia
x	Ix ¬= 2mp · [rOH · cos(θHOH/2)]2	0.75 · mprOH2
y	$I_y = 2m_p \cdot [r_{OH} \cdot \sin(\theta_{HOH}/2)]^2$	$1.25 \cdot m_p r_{OH}^2$
z	$I_z = 2m_p \cdot r_{OH}^2$	$2.00 \cdot m_p r_{OH}^2$

Table 1: Momentum of inertia [the oxygen nuclei serve as the rotation centres (centre of gravity)].

In accordance with the equipartition law of energy, the average energy of k_BT /2 is assigned to each degree of rotational and translational freedom of the water sphere, as expressed by Eqs. (2.2a) and (2.2b), respectively, where T is the temperature in Kelvin (K) and k_B is the Boltzmann constant (1.38×10−23 J/K) [9].

$$\frac{1}{2} M \left\langle \left(\frac{dx}{dt} \right)^2 \right\rangle = \frac{1}{2} k_B T \quad (2.2.a)$$

$$\frac{1}{2} I \left\langle \left(\frac{d\theta}{dt} \right)^2 \right\rangle = \frac{1}{2} k_B T \quad (2.2.b)$$

where, t, x, and θ are the time, translational and rotational displacements, respectively, and $(1/2)M\langle(dx/dt)^2\rangle$ and $(1/2)I\langle(d\theta/dt)^2\rangle$ are the time-averaged translational and rotational energies, respectively. The average thermal velocity $V_{th} = \langle dx/dt \rangle$ and angular velocity $\Omega_{th} = \langle d\theta/dt \rangle$ at 20 °C are calculated to be V_{th} = 367 m/s $(=(k_BT/M)^{1/2})$ and Ω_{th}

¬=1.41 × 10 rad/s (=$(k_BT/I)^{1/2}$), respectively. Assuming that a_w = 1.44 □,10,13 the thermal rotation velocity V_{th},s on the sphere surface calculated using Ω_{th} is 2027 m/s (= Ω_{th} ▪ a_w), which is proportional to $(M/2m_p)^{1/2}$ and 5.5 times V_{th}. The centrifugal force F_H acting on the rotating two hydrogen nuclei is approximately given as F_H= $2k_BT/ r_{OH}$ because F_H is calculated to be $2m_pV_{th},s^2/r_{OH}$. Irrespective of MW, the same amount of energy k_BT is assigned to the rotational energy around one rotation axis according to Eq.(2.2b). The centrifugal force F_H causes the gyro effect that keeps the same direction of the motion.

Consider a water sphere of radius a_w, and perform a rotational motion with rotational velocity dθ/dt in a Newtonian fluid of liquid water, of which viscosity is η. The rotational motion of the water sphere carrying out a random walk in the rotational direction is called rotational Brownian motion (RBM) [4,7-9]. Because the force couple for the rotational motion is $8\pi a_{w^3}\eta(d\theta/dt)$, $8\pi a_w{}^3\eta(d\theta/dt)$, the rotational motion of the water sphere is described by the Navier–Stokes equation using Eq. (2.1), which is a torque equation as [8-10]

$$I\frac{d^2\theta}{dt^2} = -8\pi a_w{}^3\eta\frac{d\theta}{dt} + F_\theta(t)a_w \qquad (2.3)$$

Where $F_\theta(t)a_w$ is an impulsive torque arising from the thermal agitation. By multiplying both sides of Eq. (2.3) by θ, Eq. (2.3) is transformed into Eq. (2.4):

$$\frac{I}{2}\frac{d^2(\theta^2)}{dt^2} - I\left(\frac{d\theta}{dt}\right)^2 = -\frac{8\pi\eta a_w{}^3}{2}\frac{d(\theta^2)}{dt} + \theta F_\theta(t)a_w \quad (2.4)$$

Where $2\theta(d^2\theta/dt^2) = d^2(\theta^2)/dt^2 - 2(d\theta/dt)^2$ is used. Taking the time average of Eq. (2.4) and using the equipartition law of Eq. (2.2b), we obtain

$$\frac{I}{2}\frac{d^2(\langle\theta^2\rangle)}{dt^2} + \frac{8\pi\eta a_w{}^3}{2}\frac{d(\langle\theta^2\rangle)}{dt} = k_BT + \langle\theta F_\theta(t)a_w\rangle \quad (2.5)$$

Where terms in brackets < > mean time-averaged quantities. Because $F_\theta(t)$ and θ independently vary with time and $F_\theta(t)$ is caused by random collisions, we obtain $\langle\theta F_\theta(t)aw\rangle = \langle\theta\rangle\langle F_\theta(t)\rangle aw$, where $\langle F_\theta(t)\rangle = 0$. Thus, $\langle\theta F_\theta(t)a_w\rangle$ in Eq. (2.5) is eliminated by time averaging. Therefore, the solution of Eq. (2.5) is

$$\frac{d(\langle\theta^2\rangle)}{dt} = \frac{2k_BT}{8\pi a_w\eta} + Ce^{-(t/\tau_p)}, \tau_p = \frac{I}{8\pi\eta a_{w^3}}, \quad (2.6)$$

Where C is a constant of integration. The inspection of Eq. (2.3) gives τp the time step of one rotational random walk as $\tau_p = I/(8\pi\eta a_w{}^3)$. The last term $Cexp(-t/\tau p)$ in Eq. (2.6) disappears for a long timescale because τ_p is of femtosecond order. Thus, the cumulative effect of the rotational random walk $\langle\theta^2\rangle$ derived from Eq. (2.6) leads to the dielectric relaxation formula (DRF) as

$$\langle\theta^2\rangle = 2D_{rot}t, D_{rot} = \frac{k_BT}{8\pi\eta a_w^3}, \text{and } \tau_{rel} = \frac{4\pi\eta a_w^3}{k_BT}, \quad (2.7)$$

Where D_{rot} is called the rotational diffusion coefficient. The time required for the rotation to change to an entirely new state is defined as the dielectric relaxation time $\tau_{rel} = 4\pi\eta a_w{}^3 / k_BT$ by setting $\langle\theta^2\rangle = 1$.

$$\tau_{rel} = 4\pi\eta a_w^3 \Big/ k_BT$$

Consider a water sphere of radius aw and mass M, and perform a translational motion in the x-direction with velocity dx/dt in a Newtonian fluid with viscosity η. The translational motion of the water sphere carrying out a random walk due to the thermal agitation is called translational Brownian motion [3,4,6,7]. Stokes' law gives the resistive drag (RD) for the translational motion as $6\pi a_w\eta(dx/dt)$ [1,2]; thus, the translational motion of the water sphere is described by the Navier–Stokes equation as: [9,10]

$$M\frac{(d^2x)}{(dt^2)} = -6\pi a_w\eta\frac{dx}{dt} + F_x(t), \quad (2.8)$$

Where $F_x(t)$ is time and a impulsive force arising from random collisions, respectively. Using Eq. (2.1), the solution of Eq. (2.8) is derived as

$$\frac{d(\langle x^2\rangle)}{dt} = \frac{2k_BT}{6\pi a_w\eta} + Ce^{-(t/\tau_w)}, \tau_w = \frac{M}{6\pi a_w\eta}, \quad (2.9)$$

Where C is a constant of integration. The inspection of Eq. (2.8) gives τw the time step of one translational random walk as $\tau_w = M/(6\pi\eta a_w)$. The last term $Cexp(-t/\tau_w)$ in Eq. (2.9) disappears for a long timescale because τ_w is of femtosecond order. Thus, the cumulative effect of the translational random walk $\langle x^2\rangle$ in Eq. (2.9) leads to the translational diffusion described by the Stokes–Einstein equation (SEE):

$$\langle x^2\rangle = 2Dt, D = \frac{(k_BT)}{6\pi\eta a_w}, \quad (2.10)$$

Where D is the diffusion coefficient of the translational Brownian motion.

The RD in the SEE [$6\pi a_w \eta(dx/dt)$] and the force couple in the RDF [$8\pi a_w^3 \eta(d\theta/dt)$] are approximately equivalent, because RBM can be regarded as small particles carrying out random walks on a molecular surface being affected by the RD in a manner similar to Stokes' law used in the SEE. Thus, the factors $6\pi a_w \eta$ and $8\pi a_w^3 \eta$ in the denominators of the SEE and DRF, respectively, are also referred to as the RD. The difference between [$6\pi a_w \eta(dx/dt)$] in TBM and [$8\pi a_w^3 \eta(d\theta/dt)$] in RBM is that [$6\pi a_w \eta(dx/dt)$] has two components of the viscous drag: [$4\pi a_w \eta(dx/dt)$] and pressure force:[$4\pi a_w \eta(dx/dt)$] while [$8\pi a_w^3 \eta(d\theta/dt)$] has only a single component of the viscous drag.1

The translational displacement x_{tra} for one translational random walk time step τ_w is $x_{tra} = V_{th} \cdot \tau_w$. Because the repetition number N of the random walk after time t is given as $N = t/\tau_w$, N repetitions with random displacement x_{tra} lead to an average displacement of $\langle x^2 \rangle = N \langle x_{tra} \rangle^2$ (= $tV_{th}^2 \tau_w$), which is expressed as

$$\left\langle x^2 \right\rangle = \frac{k_B T}{6\pi a \eta} \hat{o}_w t \ , \hat{o}_w = \frac{M}{6}_w \ . \quad (2.11)$$

Thus, we obtain $\langle x^2 \rangle = D_{trans} t$, where $D = k_B T/6\pi a \eta$, which is similar to Eq. (2.6). Therefore, except for the numeric factor of 2, the SEE can be derived approximately without solving Eq. (2.2). Similarly, the angle displacement δ for one rotational random walk duration τ_p is $\delta = \Omega_{th} \cdot \tau_p$. Because the repetition number N of the rotational random walk after time t is given as $N = t/\tau_p$, N repetitions with random displacement δ lead to an average angle displacement of $\langle \theta^2 \rangle = N \langle \delta \rangle^2$ (= $t\Omega_{th}^2 \tau_p$), which is expressed as

$$\left\langle \theta^2 \right\rangle = \frac{k_B T}{8\pi a^3 \eta} \hat{o}_p t \ , \hat{o}_p = \frac{I}{8}^3_w \ . \quad (2.12)$$

Thus, we obtain $\langle \theta^2 \rangle = D_{rot} t$, where $D_{rot} = k_B T/8\pi a_w^3 \eta$, which is similar to Eq. (2.7). Therefore, except for the numeric factor of 2, the DRF can be derived approximately without solving Eq. (2.3).

Because the time steps τ_p and τ_w of the translational and rotational random walks τ_p and τ_w are calculated to be τ_p = 0.271 fs and τ_w = 11.1 fs at 20 C, respectively. The ratio τ_w / τ_p is 41, which is proportional to the mass ratio M / m_p (=18) and does not depend on T. The translational Brownian motion turns the direction every 41 rotations because $\tau_w : \tau_p$ = 41:1. The kinetic energies of the molecule performing TBM and RBM are indicated by E_{trans} and E_{rot}, respectively. Because the stride of one translational random walk is $V_{th} \cdot \tau_w$, and RD is $6\pi a_w \eta V_{th} (= M \cdot V_{th}/\tau_w)$ [1,2] the energy consumed per one time step τ_w of TBM is $k_B T$ (= $V_{th}^2 \cdot M$). Because the angle displacement of one rotational random walk is $\Omega_{th} \cdot \tau_p$ and force couple is $8\pi a_w^3 \eta \Omega_{th}$ (= $I \cdot \Omega_{th} / \tau_p$), the energy consumed per one time step τ_p of RBM is $k_B T$ (= $\Omega_{th}^2 \cdot I$). Thus, the E_{trans} and E_{rot} have the maximum energies of $E_{trans,max} = E_{rot,max} = k_B T$ at the start of the random walk of t= 0 and decreases monotonically to the minimum energies of $E_{trans,min} = E_{rot,min} = 0$ at the end of one random walk of $t = \tau_w$ and τ_p, respectively. Despite the monotonic decrease of E_{rot} during τ_p, the rotational random walk consumes 41 times more energy than translational random walk during a single translational random walk time step τ_w.

Sphere Radii of H_2O and D_2O Determined from Dielectric Relaxation Time

When the volumetric radius of the water sphere is assumed to be a_{vol}, the volume of the water sphere is given by $4\pi a_{vol}^3 / 3$. The number N of water spheres existing in 1.0 m^3 is $1/(4\pi a_{vol}^3 / 3)$, which is equivalent to the density ρ divided by the mass of one molecule. Thus, the sphere radii ${}^H a_{vol}$ and ${}^D a_{vol}$ of H_2O and D_2O are calculated from $1/(4\pi {}^H a_{vol}^3 / 3) = {}^H\rho / 18 m_p$, and $1/(4\pi {}^D a_{vol}^3 / 3) = {}^D\rho / 20 m_p$, where ${}^H\rho$ and ${}^D\rho$ are the liquid densities of H_2O and D_2O, respectively. The ${}^H a_{vol}$, ${}^H\rho$ and ${}^D a_{vol}$, ${}^D\rho$ as functions of T in °C at 1 atm are shown on the right side in Tables 2-5, respectively, where the decrease of ${}^H\rho$ and ${}^D\rho$ with T and increase of ${}^H a_{vol}$ and ${}^D a_{vol}$ with T are recognized. The increases of ${}^H a_{vol}$ and ${}^D a_{vol}$ with T can be regarded as the thermal expansion of the sphere volume served for the rotations of H_2O and D_2O molecules although the molecular radius determined by the electron cloud does not expand with T. Because ${}^H\rho$ and ${}^D\rho$ take their maximums exactly at 3.98 °C and at 11.6°C, respectively, the maximum densities of ${}^H\rho_{max}$ and ${}^D\rho_{max}$ are approximately set to be ${}^H\rho$ at 0°C and ${}^D\rho$ at 10°C, respectively. The minimum volumetric radii of ${}^H a_{vol,min}$ and ${}^D a_{vol,min}$ are set to be ${}^H a_{vol,min}$ = 1.9253 Å at 0°C and ${}^D a_{vol,min}$ = 1.9282Å at 10 °C, respectively. The thermal expansion rates of the volumetric radii ${}^H a_{vol}$ and ${}^D a_{vol}$ are defined as $({}^H a_{vol} / {}^H a_{vol,min})$ and $({}^D a_{vol} / {}^D a_{vol,min})$, which are calculated from $({}^H\rho_{max} / {}^H\rho)1/3$ and $({}^D\rho_{max} / {}^D\rho)^{1/3}$, respectively. The rates of $({}^H\rho_{max} / {}^H\rho)^{1/3}$ and $({}^D\rho_{max} / {}^D\rho)^{1/3}$ as functions of T are shown in Tables 2-5 and Figure 2-5. Although $({}^H\rho_{max} / {}^H\rho)^{1/3}$ and $({}^D\rho_{max} / {}^D\rho)^{1/3}$ are not exactly proportional to T, the thermal expansion rates vol of H_2O from 0 to 50°C and D_2O from 10 to 50°C are calculated to be vol = 7.9×10-5 /°C. The calculation based on the hexagonally close-packed H_2O sphere yields that the H_2O radius a_{hex} is 1.74 Å.13 because the water sphere is not close-packed, ${}^H a_{vol}$ is greater than a_{hex}. The sphere radius having the degree of rotational freedom for RBM is smaller than a_{vol} and a_{hex}, which will be determined later.

Quantity	Temperature	Viscosity	Diffusion Coefficient	Stokes Radius	Radius Expansion	Ratio	Thermal Expansion Rate	Volumetric Radius	Density *
Symbol Unit	T□	$^{H}\eta$ (10^{-3}) Pa·s	τ_{rel} (10^{-12}) s	$^{H_2O}a_w$ □	$^{H_2O}a_w$/ $^{H_2O}a_{w,in}$	**	($^{H}\rho_{max}$/$^{H}\rho$)$^{1/3}$	$^{H}a_{vol}$ □	$^{H}\rho$ (10^3) kg/m^3
	0	1.7930	17.8	1.439	1.000000	----	1.000000	1.9253	0.99984
	10	1.3070	12.7	1.446	1.004864	104.2	1.000047	1.9254	0.99970
	20	1.0020	9.55	1.453	1.009729	17.88	1.000544	1.9264	0.99821
	30	0.7977	7.37	1.454	1.010424	7.35	1.001418	1.9280	0.99565
	40	0.6532	5.94	1.462	1.015983	6.26	1.002553	1.9302	0.99222
	50	0.5470	4.84	1.464	1.017373	4.38	1.003969	1.9330	0.98803
	60	0.4665	4.04	1.467	1.019458	3.47	1.005610	1.9361	0.98320
	70	0.4040					1.007465	1.9397	0.97778
	75	0.3780	3.22	1.482	1.029882	3.53	1.008466	1.9416	0.97487
	80	0.3780					1.009520	1.9436	0.97182

Table 2: Temperature dependence of the sphere radius of H_2O calculated using the dielectric relaxation time τrel measured in 1948.

*

$$\left[{}^{H_2O}a_w / {}^{H_2O}a_{w,min} - 1 \right] / \left[\left({}^{H}\rho_{max} / {}^{H}\rho \right)^{1/3} - \right]$$

**

$$\left[{}^{H_2O}a_w / {}^{H_2O}a_{w,min} - 1 \right] / \left[\left({}^{H}\rho_{max} / {}^{H}\rho \right)^{1/3} - \right]$$

Quantity	Temperature	Viscosity	Diffusion Coefficient	Stokes Radius	Radius Expansion	Ratio	Thermal Expansion Rate	Volum etric Radius	Density
Symbol Unit	T□	$^{H}\eta$ (10^{-3}) Pa·s	τ_{rel} (10^{-12}) s	$^{H_2O}a_w$ □	$^{H_2O}a_w$/$^{H_2O}a_{w,in}$	[$^{H_2O}a_w$/ $^{H_2O}a_{w,min}$ -1] /[($^{H}\rho_{max}$/ $^{H}\rho$)$^{1/3}$ -1]	($^{H}\rho_{max}$/ $^{H}\rho$)$^{1/3}$	$^{H}a_{vol}$ □	$^{H}\rho$ (10^3) kg/m^3
	0	1.7930	17.9	1.441	1.000000	-----	1.000000	1.9253	0.99984
	10	1.3070	12.6	1.442	1.000694	14.9	1.000047	1.9254	0.99970
	20	1.0020	9.3	1.440	0.999306	-1.28	1.000544	1.9264	0.99821
	30	0.7977	7.2	1.443	1.001388	0.979	1.001418	1.9280	0.99565
	40	0.6532	5.8	1.451	1.006940	2.72	1.002553	1.9302	0.99222
	50	0.5470	4.8	1.460	1.013185	3.32	1.003969	1.9330	0.98803
	60	0.4665	3.9	1.450	1.006246	1.11	1.005610	1.9361	0.98320
	70	0.4040					1.007465	1.9397	0.97778
	75	0.3780	3.2	1.479	1.026371	3.11	1.008466	1.9416	0.97487
	80	0.3780					1.009520	1.9436	0.97182

Table 3: Temperature dependence of the sphere radius of H_2O calculated using the dielectric relaxation time τrel measured in 1972.

Quantity	Temperature	Viscosity	Diffusion Coefficient	Stokes Radius	Radius Expansion	Ratio	Thermal Expansion Rate	Volumetric Radius	Density
Symbol Unit	T□	$^{H}\eta$ (10^{-3}) Pa·s	τ_{rel} (10^{-12}) s	$^{H_2O}a_w$ □	$^{H_2O}a_w/^{H_2O}a_{w,in}$	[$^{H_2O}a_w/^{H_2O}a_{w,min}$ -1] /[$(^{H}\rho_{max}/^{H}\rho)^{1/3}$ -1]	$(^{H}\rho_{max}/^{H}\rho)^{1/3}$	$^{H}a_{vol}$ □	$^{H}\rho$ (10^3) kg/m^3
	5	1.996	20.4	1.462	1.005502	91.2	1.000060	1.9283	1.1058
	10	1.679	16.6	1.454	1.000000	-----	1.000000	1.9282	1.1060
	20	1.247	12.3	1.470	1.011004	52.1	1.000211	1.9286	1.1060
	30	0.972	9.34	1.473	1.013067	15.4	1.000845	1.9298	1.1032
	40	0.785	7.21	1.467	1.008941	4.85	1.001845	1.9317	1.0999
	50	0.651	5.89	1.475	1.014443	4.58	1.003154	1.9343	1.0956
	60	0.552	4.90	1.481	1.018569	3.94	1.004716	1.9373	1.0905

Table 4: Temperature dependence of the sphere radius of D_2O calculated using the dielectric relaxation time τ_{rel} measured in 1948.

Quantity	Temperature	Viscosity	Diffusion Coefficient	Stokes Radius	Radius Expansion	Ratio	Thermal Expansion Rate	Volumetric Radius	Density
Symbol Unit	T°C	$\eta(10^{-3})$ Pa·s	D(10^{-9}) m^2/s	^{H2O}a Å	Rate $^{H2O}a/^{H2O}a_{min}$	[$^{H2O}a/^{H2O}a_{min}$ -1] / [$(^{H}\rho_{max}/^{H}\rho)^{1/3}$ -1]	$(^{H}\rho_{max}/^{H}\rho)^{1/3}$	$^{H}a_{vol}$ Å	$^{H}\rho$ (10^3) kg/m^3
	5.29	1.520	1.309	1.025	1.000	----	1.000000	1.9252	0.999959
	15.01	1.138	1.751	1.059	1.033	113	1.000292	1.9258	0.999084
	25.00	0.890	2.275	1.078	1.052	53. 3	1.000974	1.9271	0.997044
	39.98	0.653	3.186	1.102	1.075	28. 9	1.002597	1.9302	0.992210
	50.00	0.548	3.862	1.118	1.091	22. 7	1.004002	1.9330	0.988050

Table 5: Temperature dependence of the Stokes radius of H_2O calculated using the diffusion coefficient determined by tracking $H_2$18O tracer moving in H_2O.

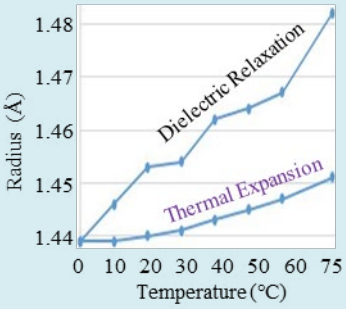

Figure 2: Sphere Radius of H_2O calculated using τ_{rel} measured in 1948.

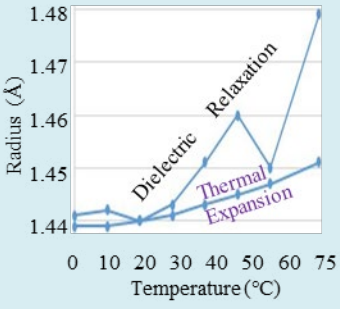

Figure 3: Sphere Radius of H_2O calculated using τ_{rel} measured in 1972.

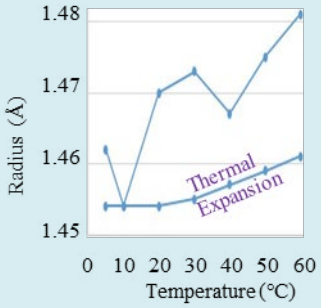

Figure 4: Sphere Radius of D_2O calculated using τ_{rel} measured in 1948.

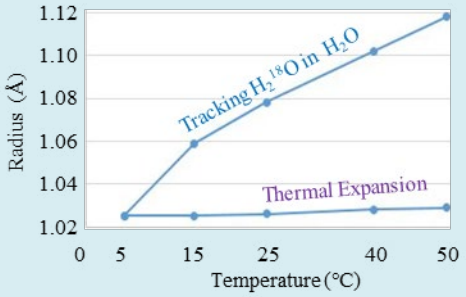

Figure 5: Stokes radius of $H_2$18O tracer diffusing in H_2O measured in 1984.

The van der Waals b constant is determined from $b = RT_c/8P_c$, where R (= N_Ak_B), N_A, k_B, T_c, and P_c are the gas constant (8.3145 J/(K・mol)), Avogadro number (6.02214×10^{23} /mol), critical temperature (K), and critical pressure (Pa), respectively [25-27]. Because Tc, and P_c are 647.3 K and 22.12×10^6 Pa (= 218.3 atm) for H_2O, and 643.89 K and 21.66×10^6 Pa (= 213.7 atm) for D_2O, bs of H_2O and D_2O are calculated to be 3.041×10^{-5} m3/mol and 3.090×10^{-5} m3/mol, respectively. Thus, the radii ${}^{H_2O}a_w{}^b$ and ${}^{D_2O}a_w{}^b$ of H_2O and D_2O in the vapour state are calculated to be ${}^{H2O}a_w{}^b$ = 1.445□ and ${}^{D2O}a_w{}^b$ = 1.453□, using $N_A(1/2)(4\pi/3)(2a_w)^3$ = b [28]. The most accurate radii ${}^{H2O}a_w{}^b$ and ${}^{D2O}a_w{}^b$ of H_2O and D_2O molecules, which are regarded as rotating spheres were determined with four-digit accuracy in the aqueous vapour state by the van der Waals b constant, where ${}^{D2O}a_w{}^b$ was greater than ${}^{H2O}a_w{}^b$ by 5.5×10^{-3}. The radii ${}^{H2O}a_w{}^b$ and ${}^{D2O}a_w{}^b$ will be the standards in the evaluation of H_2O and D_2O radii in the liquid state.

The dielectric relaxation time τ_{rel} of a polarised molecule such as a water molecule is measured by locating a molecule in an electric condenser with an alternating electric field of frequency f. The capacity of the condenser decreases above a critical frequency $f_{cr} = 1/\tau_{rel}$ because the rotational motion of the electric dipole cannot respond to a high-frequency alternating field. Thus, the dependence of the capacity on f determines τ_{rel}. Because τ_{rel} is measured by applying an alternative electric potential difference of 0.1V on the two electrodes surrounding the 30-μm-thick liquid cell that matches the THz band wave-length, the applied field E_{rel} is $E_{rel} = 3\times10^3$ V/m. If the maximum electric field E_{max} without causing chemical reactions is assumed to be E_{max} = 109 V/m (= 100 mV/Å), the applied E_{rel} will not induce chemical reactions. Because the electric force acting on the hydrogens rotating around the oxygen nucleus is qHErel, the acceleration for the velocity vH of the hydrogen by the force qHErel is q_HE_{rel}/mp. Thus, vH reaches the maximum rotation velocity $V_{H,max}$ =16 μm/s [=(q_HE_{rel}/m_p) ・ $(\tau_p/2)$] for the half of one rotational random walk time step τ_p. Because $V_{H,max}$ is as low as 7.7×10-9 of the average rotational velocity $V_{th,s}$ = 2027 m/s at 20°C, the applied field E_{rel} does not affect the accuracy of the τ_{rel} measurement.

The molecular sphere radii ${}^{H2O}a_w$ of H_2O and ${}^{D2O}a_w$ of D_2O are calculated by substituting the measured values of τ_{rel}, η, and T of H_2O and D_2O into the DRF. Respectively. The τ_{rel} [14-23,24] and η[25] of H_2O as functions of T are shown in Tables 2 and 3, and τ_{rel} [14-23] and η[25,26] of D_2O are shown in Table 4. The D_2O measurement was performed at T ≧5□ because the melting point (m.p.) of D_2O is 3.81 □. There were two τ_{rel} measurements for H_2O in 1948 (Table 2) [23] and in 1972 (Table 3) [24], and one measurement for D_2O in 1948 (Table 4) [23]. The sphere radii ${}^{H2O}a_w$ and ${}^{D2O}a_w$ of H_2O and D_2O calculated using the DRF are shown in Tables 2,3, Figs. 2,3, and Table 4, Fig. 4, respectively. The minimum radii ${}^{H2O}a_{w,min}$ and ${}^{D2O}a_{w,min}$ of H_2O and D_2O are calculated as ${}^{H2O}a_{w,min}$ = 1.44±0.01 □ at 0□ and ${}^{D2O}a_{w,min}$ = 1.45±0.01 □ at 10□ because ${}^H\rho_{max}$ and ${}^D\rho_{max}$ are defined at 0 and 10□, respectively. Because there are temperature points at which the radii change by 0.01 Å with 10°C increment in the fluctuating curves in Figs. 3 and 4, the error width in calculating ${}^{H2O}a_{w,min}$ and ${}^{D2O}a_{w,min}$ was determined to be ±0.01 Å. The radius expansion rates of the radii ${}^{H2O}a_w$ and ${}^{D2O}a_w$ are defined as $({}^{H2O}a_w / {}^{H2O}a_{w,min})$ and $({}^{D2O}a_w / {}^{D2O}a_{w,min})$, respectively. The rates $({}^{H2O}a_w / {}^{H2O}a_{w,min})$ and $({}^{D2O}a_w / {}^{D2O}a_{w,min})$ as functions of T are shown in Tables 2,3, Figs. 2,3, and Table 4, Fig. 4, respectively. Although $({}^{H2O}a_w/{}^{H2O}a_{w,min})$ and $({}^{D2O}a_w/{}^{D2O}a_{w,min})$ are not exactly proportional to T, the radius expansion rates rot of H_2O from 0 to 50°C and D_2O from 10 to 50°C are determined to be rot = $(3.0\pm0.6)\times10^{-4}$ /□, of which error width 0.6×10^{-4} /°C is determined from the fluctuated curves in Figurs 2-4. There was not sufficient accuracy for the τ_{rel} data to discriminate the difference of the radius and radius expansion rate between H_2O and D_2O.

The radius expansion rate calculated from the DRF is greater than the thermal expansion rate calculated from the density as shown in Tables 2-4 and Figs. 2-4. Thus, the ratios of the radius expansion to thermal expansion of H_2O and D_2O

are defined by [$^{H2O}a_w$ /$^{H2O}a_{w,min}$ -1] / [($^{H}\rho_{max}$/$^{H}\rho$)$^{1/3}$ -1] and [$^{D2O}a_w$ /$^{D2O}a_{w,min}$ -1] / [($^{D}\rho_{max}$/D_ρ)$^{1/3}$ -1], respectively. These ratios are shown at the centre in Tables 2-4, where they cannot be defined for H_2O at 0□ and for D_2O 10□. Although the ratios are fluctuating because the curves in Figs. 2-4 are fluctuating, the rates are almost converged to stable values of 3.53 and 3.11 at the highest τrel measurement temperatures of 75°C for H_2O in Figures 2 and 3, respectively, and that of 3.94 at 60°C for D_2O in Figure 4. These ratios mean that the radius expansion with temperature for H_2O and D_2O calculated using the DRF is about four times greater than the thermal expansion calculated using the density.

Because τ_{rel} is 9.55 ps at 20□, the ratio τ_{rel} :τ_w :τ_p is calculated to be 35000:41:1 at 20°C. The ratio means that there are sufficient number of rotations to obtain the stable statistical average during one dielectric relaxation because τ_{rel} :τ_p = 35000:1. The translational random walk changes the direction every 41 rotations because τ_w :τ_p = 41:1. The solvent viscosity mainly affects the accuracy in calculating the molecular radius using the DRF. If the viscosities of H_2O and D_2O at the maximum density temperatures are determined with three- to four-digit accuracy, the calculation using the DRF can discriminate the difference of the sphere radii between H_2O and D_2O in the liquid state because the van der Waals b constant determined that $^{D2O}a_w{}^b$ was greater than $^{H2O}a_w{}^b$ by 5.5×10^{-3}.

The Stokes radius ^{H2O}a of H_2O is calculated by substituting the measured values of D, η, and T of H_2O into the SEE. The values of D [30] and η [25] of H_2O from 5.29°C to 50°C are shown in Table 5. The Stokes radius ^{H2O}a calculated using the SEE is shown in Table 5 and Figure 5. The D of H_2O was measured by tracking the tracer $H_2{}^{18}O$ as solute moving in H_2O as solvent [30]. Although tracer tracking cannot measure ^{self}D, the obtained D of $H_2{}^{18}O$ in H_2O is regarded as the ^{self}D of H_2O. The minimum Stokes radius $^{H2O}a_{min}$ is 1.025 Å at 5.29°C. The radius expansion rate of (^{H2O}a / $^{H2O}a_{min}$) as a function of T is shown in Tables 5. Although (^{H2O}a / $^{H2O}a_{min}$) is not exactly proportional to T, the Stokes radius expansion rate Δ_{trans} of H_2O from 5.29 to 50°C is calculated to be Δ_{trans}=2.0×10^{-3}/°C. The Stokes radius expansion rate calculated using the SEE is greater than the thermal expansion rate calculated from the density as shown in Table 5 and Figure 5. The ratio of the Stokes radius expansion to thermal expansion of H_2O defined by [^{H2O}a /$^{H2O}a_{min}$ -1] / [($^{H}\rho_{max}$/$^{H}\rho$)$^{1/3}$ -1] is shown at the centre in Table 5, where they cannot be defined at 5.29°C. Although it takes an extraordinarily greater value of 113 at 15.01°C, the ratio converges to 22.7 at the highest D measurement temperature of 50°C. The ratio means that the radius expansion with temperature calculated using the SEE is 23 times greater than the thermal expansion calculated using the density.

Because the viscosities η of H_2O and D_2O are determined in increments of 10□ [25,26], the η at other temperature points should be estimated, where the lowest measurement temperature of the η of D_2O is 3.82°C. The two viscosities of H_2O (or D_2O) measured at lower T_{low} and higher T_{high} temperatures are denoted by η_{low} and η_{high} , respectively. When the temperature difference between T_{low} and T_{high} is within 10°C, η_{low} and η_{high} are described using similar two parameters of A and E as

$$\varsigma_{low} = A\exp\left(-\frac{E}{k_B T_{low}}\right) \quad (3.1a)$$

$$\varsigma_{high} = A\exp\left(-\frac{E}{k_B T_{high}}\right) \quad (3.1b)$$

Because A and E are determined from Eqs. (3.1a) and (3.1b), η at the intermediate temperature T ($T_{low} \leqq T \leqq T_{high}$) is calculated from η = Aexp(- E/k_BT). The parameter E is called the activation energy that was known to be almost constant within a temperature interval of 10□. Because η of D2O at 5□ in Table 4 and η of H_2O at 5.29, 15.01, 25.00, and 39.98□ in Table 5 are estimated using Eq. (3.1), and the curves showing the temperature dependence of the radius as shown in Figs. 2-4 are fluctuating, the expansion rates of Δ_{rot} and Δ_{trans} were determined with two digit accuracy.

There are three radius expansion rates of Δ_{vol}, Δ_{rot}, and Δ_{trans} caused by temperature increase, where Δ_{vol}= 7.9×10^{-5}/°C is the thermal expansion rate determined by the density, Δ_{rot}= 3.0×10^{-4}/□ is the radius expansion rate determined by τ_{rel}, and Δ_{trans}= 2.0×10^{-3}/□ is the Stokes radius expansion rate determined by D. The ratio among the three rates is approximately described as Δ_{vol}: Δ_{rot}: Δ_{trans} = 1:4:23. Although TBM and RBM are occurred simultaneously, an essential difference between the SEE and DRF was found because Δ_{trans} is six times greater than Δ_{rot}.

Water Sphere Radii Performing Rotational Brownian Motion During Cluster Formation

Locating a uniform medium of an air, liquid, or solid in an electric capacitor applied by dc or alternating electric field with less than 1-kHz frequency, the dielectric ratio εr per mol of the molecule in the medium is determined. The adoption of 1-kHz alternating field is to avoid the cohesion of the molecule into the electrode. Based on ε_r, the dipole moment of the molecule in the medium can be determined [8]. The similar ε_r per mol is obtained in both liquid and vapour states when the molecule has no correlations and associations. Thus, most molecules exhibit similar dipole moments in liquid and vapour states. However, the dipole moment of the

water molecule in liquid state is about twice that in vapour state. When oxygen is placed at the centre of the tetrahedron, four atomic bonds can be made toward the four apices of the tetrahedron. Two hydrogens or two deuteriums are bound to two of the four apices in H_2O and D_2O, respectively, and the remaining two apexes create two hydrogen bonds using unpaired electrons. Thus, the hydrogen-bonded cluster model composed by five water molecules in the liquid state was proposed, where four oxygens and one oxygen locate at the four vertices and one centre of the tetrahedron, respectively [31,32]. Because the hydrogen bonding is created by a hydrogen existing between two oxygens, the locations of the ten hydrogens in the tetrahedron under the restriction of the hydrogen bonding create the correlation among the water dipole moments. Because the discrepancy of the water dipole moments between the liquid and vapour states was explained by the correlation, the existence of the hydrogen-bonded cluster is accepted. The five oxygens locations constituting the tetrahedron cluster were confirmed by the X-ray scattering of liquid water [14].

The volumetric molar heat capacity C_v of a gas is determined by the total number of degrees of motional freedom N_f and is expressed as $C_v = (N_f/2)R$. The possibility of translational motion along the x-, y-, and z-axes implies three degrees of translational freedom (N_f = 3) for monatomic gases. Because of the three possible directions of the rotational axis, the x-, y-, and z-axes, imply three additional degrees of rotational freedom (giving a total of N_f = 6) for three-atom molecules such as water molecules, the isovolumic molar heat capacity of aqueous vapour (H_2O gas) is $C_v \fallingdotseq 6(R/2)$, which implies six degrees of motional freedom. Because the water sphere is regarded to be a perfect sphere similar to monatomic gases such as He, the three degrees of rotational freedom for the rotating water sphere is inconsistent. However, the experimentally confirmed C_v of H_2O vapour assures the validity of Eq. (2.2) and the three degrees of rotational freedom of H_2O vapour. The three degrees of rotational freedom are also expected to be conserved in a liquid water molecule because the molar heat capacity of water is approximately 18.2(R/2) from 0 to 100 °C at 1 atm and the degrees of motional freedom N_f of liquid water is 18.2 (> 6). The appropriateness of ${}^{H2O}a_w$ and ${}^{D2O}a_w$ as rotating sphere radii was supported by the fact that the sphere radii ${}^{H2O}a_w$ and ${}^{D2O}a_w$ determined by τ_{rel} are similar to the radii ${}^{H2O}a_w{}^b$ and ${}^{D2O}a_w{}^b$ determined by the van der Waals b constant, and lower than the volumetric sphere radii ${}^{H2O}a_{vol}$ and ${}^{D2O}a_{vol}$ by 25%.

The existence of the hydrogen-bonded cluster, that is, some type of solid nuclei remaining in the liquid state above freezing point is also supported by the smaller entropy generated by the solid-liquid transition of water. The densities of H_2O ice and D_2O ice are about 10% less than those of H_2O liquid and D_2O liquid. The fact that the maximum density temperature of H_2O liquid and D_2O liquid exists above the m.p. is explained by the fact the ice nuclei (hydrogen-bonded clusters) that lowers the density of liquid water remains at temperatures above m.p. [14]. There are two contradicting phenomena that the residual ice nuclei melts and the liquid density increases with temperature, and that the liquid density decreases with temperature due to thermal expansion. Thus, the maximum density temperature exists above m.p. by the remaining ice nuclei and thermal expansion. The part of the excess freedom over six ΔN_f = 12.2 (= 18.2 – 6) is expected to be related to the rotation of the hydrogen-bonded cluster [10]. The radius of a water molecule estimated from τ_{rel} from the m.p. to 60°C was almost similar to the electron cloud radius of a single water molecule,[14] but not of that of the water cluster, which has been proposed to exist in super cooled liquid [33]. The measurements of ε_r and τ_{rel} are conducted at frequencies of less than kHz and THz, respectively. Thus, the water molecule as a component of a hydrogen-bonded cluster in the liquid state was considered to rotate as a single water molecule in the vapour state within the picosecond timescale of τ_{rel}, while the hydrogen-bonded cluster has an averaged timescale much larger than τ_{rel}. Although the spin-lattice (T_1) and spin-spin(T_2) relaxation time scales of the NMR is the second timescale, T_1 is reasonably evaluated based on the single water molecule radius [34].

Effect of Rotational Brownian Motion on Translational Brownian Motion

The Stokes radius ${}^{H2O}a_{min}$ of H_2O is ${}^{H2O}a_{min}$ = 1.025 Å at 5.29°C, as shown in Table 5. The inaccuracy of the SEE is pointed out because ${}^{H2O}a_{min}$ = 1.025 Å is smaller than the electron cloud14 by as much as 29 % [12,13]. When a sphere of radius a is immersed in fluid, the RD required for the sphere to move with a steady velocity dx/dt is $6\pi a\eta(dx/dt)$ according to the Stokes law [1,2]. The factor $6\pi a\eta$ in the denominator of the SEE comes from $6\pi a\eta(dx/dt)$. To increase the Stokes radius of H_2O, it is proposed that the factor 6 in the SEE should be changed into a factor between 4 and 5; that is, the RD should be reduced. The inaccuracy of the SEE highlights that the Stokes radius of lower MW molecules such as water is too small when the diffusion coefficient of the low MW molecule as a solute is measured in an aqueous solution.11 The reduction in the RD is explained by the slipping condition, in which the solute molecule can easily slip through the gap between the solvent molecules when the size of the gap is compatible to that of the solute molecule.

If the factor 6 in the SEE is changed into 4.25, the Stokes radius of H_2O at 5.29°C can become 1.445Å. Thus, it is assumed that there are the active RD and inactive RD regions, where the sphere surface receives the RD and does not receive RD,

respectively, and the area ratio Γ of the inactive RD region to the entire sphere surface is given by 0.292 [= (6 - 4.25) / 6]. This means that the SEE can yield the reasonable Stokes radius for H_2O if the surrounding solvent water molecules multiplied by Γ do not contribute to the RD. The water sphere performing the Brownian motion as the solute molecule is called the centre sphere, and the water spheres surrounding the centre sphere are the solvent molecules and called the surrounding spheres. The directional axis is defined along the translational motion of the centre sphere. The cross and vertical sections are defined by planes perpendicular and parallel to the directional axis, respectively. The azimuthal angle φ_{spr}: $0° \le \varphi_{spr} \le 360°$and polar angle θ_{spr}: $0° \le \theta_{spr} \le 180°$are measured in the cross and vertical sections, respectively. The cross section is shown at the centre in Figure 6, where the directional axis is perpendicular to the paper and the centre sphere and six surrounding spheres are displayed. The circumference of the centre sphere is divided into two rubbing laminar (active RD) regions and two suction groove (inactive RD) regions, which are related to the energy transfer (consumption and supply) to the translational and rotational random walks, respectively. The angle widths of the rubbing laminar $\varphi_{spr,drg}$ and suction groove $\varphi_{spr,pls}$ regions are $\varphi_{spr,drg} = 127.5°$and $\varphi_{spr,pls} = 52.5°$, where 127.5°and 52.5°are derived from 180°×(1-Γ) and 180°×Γ, respectively. The azimuthal angles φ_{spr} covering the rubbing laminar and suction groove regions are $0° \le \varphi_{spr} \le \varphi_{spr,drg}$ and $180° \le \varphi_{spr} \le (180° + \varphi_{spr,drg})$, and $127.5° \le \varphi_{spr} \le (127.5° + \varphi_{spr,pls})$ and $(180° + 127.5°) \le \varphi_{spr} \le (180° + 127.5° + \varphi_{spr,pls})$, respectively. Four water spheres for decelerating the centre sphere as the RD and two water spheres for inducing the rotation of the centre sphere are located on the rubbing laminar and suction groove regions, respectively. The division between the two regions depends on only φ_{spr} in the cross section and not on θ_{spr} in the vertical section.

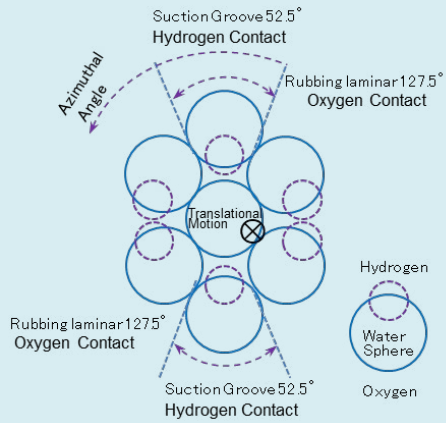

Figure 6: Rubbing laminar (active resistive drag) surface and suction groove (inactive resistive drag) surface in the cross section of the H_2O molecule performing the translational motion perpendicular to the paper.

Because the Stokes law assumes uniform laminar flow around the molecule, the uniform laminar flow cannot produce molecular rotation. Because the surface rotation velocity $V_{th,s}$ is 5.5 times greater than the translational velocity V_{th}, the molecular rotation cannot reach the necessary surface velocity $V_{th,s}$ even if the molecular rotation is induced by the directional change occurred between the two translational random walk strides with velocity V_{th}. It is difficult for the surrounding shear flow of which translational motion energy is k_BT to give the molecule performing TBM the rotational motion energy k_BT 41 times during a single translational random walk time step τ_w. The thermal energy is distributed to the translational and rotational motion freedom according to the equi-partition law in Eq. (2.2). Because the specific heat ensures the sufficient rotational freedoms in the liquid state as discussed in Section 4, the rotational energy k_BT should be recovered 41 times during τ_w, soon after the termination of the rotation. Thus, there should exist the suction groove region, where the surrounding spheres give only the rotational impulse to the centre sphere and not give the RD. The 41 times repetition of replenishing the rotational freedom with energy during one time step τ_w can be regarded as the increase of the number of the state and entropy S. One translational random walk starts when the Helmholtz free energy F = U- TS takes its local extreme due to the thermal agitation, where U is the internal energy corresponding to E_{trans} and E_{rot}. The free energy F decreases during a single time step τ_w, and recovers the local extreme as the new start of the random walk after τ_w. The translational energy dissipation of E_{tran}s and E_{rot} and rotational energy replenishment of S contribute the decrease of the free energy F during τ_w.

Collision between the same mass particles can transfer energy most efficiently. The water molecule is not exactly a perfect sphere and the two hydrogens are sticking on the water sphere surface. The rotation of the water sphere is that of the two hydrogen atoms around the oxygen nucleus as the centre of gravity. The dissipation and enhancement of the translational motion are mainly controlled by the impulse exchange between the two centres of gravity (Oxygens) of the centre and surrounding water spheres. Similarly, those of the rotational motion are mainly controlled by the impulse exchange between the two rotating hydrogens of the centre and surrounding water spheres. Although the six spheres can contact at the centre sphere surface at $\varphi_{sur} = 60°$ increments, the water sphere existing in the suction groove region cannot contact the centre sphere surface because $\varphi_{sur,pls} < 60°$. Although the distance between the centre and surrounding water spheres in the suction groove rotational impulse region is not sufficiently short to contact at their surfaces as shown in Fig. 6, the distance is sufficiently short for the rotating hydrogens to exchange impulses between the centre and surrounding spheres. The two water spheres existing in one rubbing laminar region can contact the centre sphere

surface because $\varphi_{sur,\ pls}$ > 120°. Because the oxygens of the surrounding and centre waters can contact on the surfaces in the rubbing laminar regions, the surrounding water sphere can give impulses as viscosity of the RD to the centre of gravity of the centre water sphere. If one rubbing laminar region and one suction groove region exist, the centre of gravity of the water sphere may shift in perpendicular to the directional axis due to impulses. Thus, the two rubbing laminar fluid drag regions and two suction groove regions exist face to face in symmetrical positions. Although the stride of one translational random walk $V_{th} \cdot \tau_w$ is 0.04Å at 20°C, which is less than 3% of the water sphere radius 1.44Å, and there are gaps among the centre and surrounding spheres as shown in Fig. 6, the Avogadro number average enables the area ratio Γ to divide the rubbing laminar fluid drag and suction groove regions under the smeared background assumption where the water spheres are treated as a continuous medium.

Discussion

It is possible to calculate the volume occupied by one water molecule in ice in which molecules are regularly arranged. The analysis of the molar heat capacity shows that the rotational freedom of water molecules is conserved in the liquid in which the molecules are not arranged. The facts that ice nuclei remain in the liquid water and hydrogen-bonded clusters exist above the m.p. are quantitatively estimated by the low-frequency dielectric ratio, [31,32] entropy change in solid-liquid transition, correlation among oxygen positions clarified by X-ray analysis, and maximum density temperature of 3.98°C above the m.p. of 0.00°C. Under these situations we analysed the volume of the sphere that is conserved for RBM of the liquid water molecule, of which the electron cloud is not a perfect sphere.

The sphere radii ${}^{H2O}a_w{}^b$ of H_2O and ${}^{D2O}a_w{}^b$ of D_2O in the vapour state are determined to be ${}^{H2O}a_w{}^b$ = 1.4445 Å and ${}^{D2O}a_w{}^b$ = 1.4532 Å, respectively, which are calculated using the van der Waals b constant. Although the calculation method cannot determine the temperature dependence of the sphere radius, it can be determined that the radius ${}^{D2O}a_w{}^b$ of D_2O is greater than that ${}^{H2O}a_w{}^b$ of H_2O by 0.55% because the method has four-digit accuracy. The sphere radii ${}^{H2O}a_w{}^b$ and ${}^{D2O}a_w{}^b$ calculated using the van der Waals b constant could become the basis of the sphere radii of H_2O and D_2O, respectively, despite the fact that these molecules are not perfect spheres.

When the molecules in the liquid state can be assumed to be spheres, the radius of the sphere, which is called the volumetric radius a_{vol} was calculated using the liquid density changing with temperature. The minimum volumetric radii ${}^{H2O}a_{vol,min}$ of H_2O at 0°C and ${}^{D2O}a_{vol.min}$ of D_2O at 10 °C were 1.9253 Å and 1.9282 Å, respectively. The thermal expansion rates vol of ${}^{H2O}a_{vol}$ of H_2O from 0 to 50°C and ${}^{D2O}a_{vol}$ of D_2O from 10 to 50°C were calculated to be vol =7.9×10^{-5} /°C. The ${}^{D2O}a_{vol.min}$ is greater than ${}^{H2O}a_{vol,\ min}$ by 0.15%. Although the 0.15% difference between ^{D2O}avol.min and ${}^{H2O}a_{vol,min}$ is less than the 0.55% difference between ${}^{H2O}a_w{}^b$ and ${}^{D2O}a_w{}^b$, it was determined that the D_2O sphere radius is larger than the H_2O sphere radius by the order of 0.1%. The thermal expansion rate vol =7.9×10^{-5} /°C could become the basis of the radius expansions of H_2O and D_2O with temperature in the measurements using RBM and TBM.

The sphere radii ${}^{H2O}a_w$ of H_2O and ${}^{D2O}a_w$ of D_2O were calculated to be 1.44±0.01 Å at 0°C and 1.45±0.01 Å at 10°C by substituting dielectric relaxation time τrel, viscosity η, and temperature T into the DRF. Because ${}^{H2O}a_w$ and ${}^{D2O}a_w$ change with temperature, and 0°C and 10°C are close to the maximum density temperatures of 3.98 °C for H_2O and 11.6 °C for D_2O, respectively, ${}^{H2O}a_w$ of H_2O at 0°C and ${}^{D2O}a_w$ of D_2O at 10°C became the basis of the sphere radii of H_2O and D_2O performing rotational Brownian motion (RBM) in the liquid state. The radius expansion rates rot of H_2O from 0 to 50°C and D_2O from 10 to 50°C were found to be rot =$(3.0\pm0.6)\times10^{-4}$ /°C. Because the dielectric relaxation time measurements were conducted for comparing the orientation characteristics of H_2O and D_2O molecules in liquid and various ice crystal structures and not for calculating the sphere radii, the temperature dependence of the calculated radii of H_2O and D_2O showed fluctuating curves. The error width ±0.01Å in ${}^{H2O}a_w$ at 0°C and ${}^{D2O}a_w$ at 10°C, and that ±0.6×10-4 /°C in the radius expansion rate rot are determined by the fluctuating curves. Thus, the dielectric relaxation time measurement did not have a sufficient accuracy to discriminate the sphere radius difference between H_2O and D_2O. Because the sphere radii ${}^{H2O}a_w$ at 0°C and ${}^{D2O}a_w$ at 10°C are close to ${}^{H2O}a_w{}^b$ and ${}^{D2O}a_w{}^b$, respectively, the sphere radii performing RBM in the liquid state were found to be similar to those of a single molecule in the vapour state, which is determined by the van der Waals b constant. The dielectric relaxation time τrel measurement in the picosecond time scale was found not to be affected by the hydrogen-bonded cluster having longer time scale. The rotational freedom in the liquid water molecule supported by the molar heat capacity 18.2(R/2) was also supported by the relations of ${}^{H2O}a_w < {}^{H2O}a_{vol}$ and ${}^{D2O}a_w < {}^{D2O}a_{vol}$.

Because the van der Waals b constant showed that ${}^{D2O}a_w{}^b$ is greater than ${}^{H2O}a_w{}^b$ by 0.55 %, and the liquid density showed that ${}^{D2O}a_{vol.min}$ is greater than ${}^{H2O}a_{vol,min}$ by 0.15%, the possibility to discriminate the radius difference between H_2O and D_2O by the calculation using the DRF was investigated. The rotational acceleration by the electric field can be ignored because the accelerated rotational velocity was as low as 10-9 of the thermal rotational velocity. The calculation of ${}^{D2O}a_{w,\ min}$ at 5°C using the DRF as shown in Table 4 may contain a certain error because the viscosity of D_2O at 5°C was determined from the interpolation of the

η of D_2O between 3.81°C and 10°C using Eq. (3.1) [25,26]. The apparent factor to lower the accuracy in calculating the molecular radius using the DRF is the solvent viscosity. If the viscosities of H_2O at 3.98°C and D_2O at 11.6°C, which are the maximum density temperatures, are determined with three- to four-digit accuracy, the sphere radii of H_2O and D_2O in the liquid state will be discriminated using the DRF.

The distance of the translational motion during one time step τ_p of rotation is given as $V_{th} \cdot \tau_p$. Assuming that the translational random walk changes the direction within the distance $V_{th} \cdot \tau_p$, the centrifugal force F_w acting on the centre of gravity is given as $F_w = k_B T/(V_{th} \cdot \tau_p)$ [$= MV_{th}^2/(V_{th} \cdot \tau_p)$] when the translational motion changes the direction by 90°, while the centrifugal force F_H acting on the rotating hydrogen is $F_H = 2k_B T/r_{OH}$. The ratio F_H/F_w is derived as $F_H/F_w = 2(V_{th} \cdot \tau_p)/r_{OH}$ and numerically calculated to be 2.08×10^{-3} [$= 2 \cdot 367 \cdot 0.271\times10^{-15}/0.9575\times10^{-10}$] at 20°C, which is the gyro effect that the molecular rotation impedes the course change of the translational random walk. Thus, the accuracy of the DRF may be affected by the gyro effect with 10^{-3} order.

The Stokes radius H_2Oa of H_2O is calculated by substituting the diffusional coefficient D, η, and T into the SEE. The Stokes radius expansion rate trans was 2.0×10^{-3} /°C. Although η at 0 °C is three times as large as that at 50 °C, the radius increments from 0 to 50°C due to the expansion rates of rot and trans are as low as 1.5% [$= (50\text{-}0) \times 3.0\times10^{-4}$] and 10 % [$= (50\text{-}0) \times 2.0\times10^{-3}$], respectively. However, it was pointed that Walden's law does not hold in the SEE because the 10% increment of the Stokes radius is too great in comparison with the radius increment 0.4% [$= (50\text{-}0) \times 7.9\times10^{-5}$] due to thermal expansion rate vol [11-13]. It can be assumed that Walden's law holds in the DRF if the 1.5% increment of the sphere radius is allowable, which is four times greater than that due to the thermal expansion rate vol. Although RBM and TBM occur simultaneously, an essential difference in evaluating the water radius between RBM and TBM was found because trans is six times as large as rot. Even if rot is smaller than trans, a problem of the DRF remains that rot is four times as large as the thermal expansion vol.

Stokes' law is applicable to the EPF because the electrophoretic velocity v_{ep} is faster than the thermal velocity and the electric energy inducing the v_{ep} is supplied from the outside of the system. However, there is a possibility that a finite part of the sphere surface cannot receive the RD described by Stokes' law when the molecular sphere receives both impulses to increase and decrease the translational and rotational motion energies from the surrounding solvent. Thus, the surface of the water sphere performing TBM was divided into the rubbing laminar fluid drag (active RD) and suction groove (inactive RD) regions in order to reduce the RD in the denominator of the SEE. It was expected that the Stokes radius of water calculated using the SEE increases up to a reasonable value due to the reduction of the RD caused by the suction groove region where the water sphere receives the rotational energy 41 times during one translational random walk time step and does not receive the RD for decelerating the translational motion. Although the suction groove region is too narrow for the two water spheres to contact on their surfaces, the exchange of the rotational energy between the surrounding and centre water molecules is efficiently performed through contacts between rotating hydrogens protruding from the water sphere surface. The energy supply to the rotational freedom during one translational random walk determined the reduction rate of the RD. The division of the molecular sphere into the active and inactive RD regions was expected to improve the inaccuracy of the SEE without using the slipping condition. Because the SEE also has the inaccuracy that the Stokes radius varies with temperature, detailed investigations on the SEE will be reported later.

Conclusions

The molecular sphere radii of H_2O and D_2O in the liquid state to achieve rotational Brownian motion were found to be similar to those in the vapour state because those calculated using the dielectric relaxation formula (DRF) matched the radii calculated using van der Waals b constant. The Stokes radius of H_2O is calculated using the Stokes-Einstein equation (SEE), which relates the molecular radius with the diffusion coefficient in translational Brownian motion. The thermal expansion rate of the water sphere radius is calculated using the liquid density decrease with temperature from 0 to 50°C. The advantage of the use of the DRF in the calculation of the water sphere radius was confirmed because the radius expansion rate calculated using the DRF is much closer to the thermal expansion rate than that calculated using the SEE.

Acknowledgement

T.O. is grateful to the late Dr. T. Yasuda a Professor Emeritus of Tokyo Institute of Technology for his insightful contributions.

Competing Interests

I have no competing interests.

Funding

There is no funding.

References

1. Lamb H (1932) Hydrodynamics.
2. Batchelor GK (1967) An Introduction to Fluid Dynamics.

Cambridge University Press 14(2): 364-368.

3. Robinson RA, Stokes RH (1955) Electrolyte Solutions.
4. Shaw DJ (1980) Introduction to Colloid and Surface Chemistry.
5. Robert LK (1973) Ionic Transport in Water and Mixed Aqueous Solvents, Water—A Comprehensive Treatise 3: 174-209.
6. Einstein A (1956) Investigations on the theory of the Brownian motion.
7. Perrin J (1990) Atoms.
8. Debye P (1929) Polar Molecules, pp: 84.
9. Kubo R, Ichimura H, Usui T, Hashitsume N (1999) Statistical Mechanics.
10. Osuga T, and Tatsuoka H (2009) Magnetic-field transfer of water molecules. J App Phys 106: 094311.
11. Longsworth LG (1954) Diffusion in the Water—Methanol System and the Walden Product. J Phys Chem 58(9): 770.
12. Defries T, Jonas J (1977) Molecular motions in compressed liquid heavy water at low temperatures. J Chem Phys 66(12): 5393.
13. Krynicki K, Green CD, Sawyer DW (1978) Pressure and temperature dependence of self-diffusion in water Faraday Discuss. Chem Soc 66: 199.
14. Eisenberg D, Kauzmann W (1969) The Structure and Properties of water, pp: 21.
15. Steere RL, Ackers GK (1962) Restricted-diffusion Chromatography through Calibrated Columns of Granulated Agar Gel; A Simple Method for Particle-Size Determination. Nature 196: 475-476.
16. Jenner CF, Xia Y, Eccles CD, Callaghan PT (1988) Circulation of water within wheat grain revealed by nuclear magnetic resonance microimaging. Nature 336: 399-402.
17. Yamasaki F, Kurisu K, Kenichi S, Kazunori A, Kazuhiko S, et al. (2005) Apparent Diffusion Coefficient of Human Brain Tumors at MR Imaging. Radiology 253(3): 985-991.
18. Cummins HZ, Pike ER (1974) editors Photon correlation and light beating spectroscopy.
19. Onsager L, Fuoss RM (1932) Irreversible Processes in Electrolytes. Diffusion, Conductance and Viscous Flow in Arbitrary Mixtures of Strong Electrolytes. J Phys Chem 36(11): 2689-2778.
20. Osuga T, Han S (2004) Proton magnetic resonance imaging of diffusion of high- and low-molecular-weight contrast agents in opaque porous media saturated with water. Magn Reason Imaging 22(7): 1039-1042.
21. Osuga T, Ikehira H, Weerakoon B (2017) Diffusion coefficient measurements of T1-enhanced contrast agents in water using 0.3 T spin echo proton MRI. Nanomedicine & Nanotechnology Open Access 2(2) 000122.
22. Holmes WM, Maclellan S, Condon B, Dufès C, Evans TRJ, et al. (2007) High-resolution 3D isotropic MR imaging of mouse flank tumours obtained in vivo with solenoid RF micro-coil. Physics in medicine and biology 53(2): 505.
23. Collie EH, Hasted JB, Ritson DM (1948) Proc Phys Soc 60(2): 145.
24. Hasted JB (1972) The Water Molecule, Water—A Comprehensive Treatise. F Franks 1: 277.
25. Haynes WM, Lide DR, Bruno TJ (2013) CRC Handbook of Chemistry and Physics 93rd ed. CRC Press, pp: 2664.
26. Matsunaga N, Nagashima A (1983) Transport Properties of Liquid and Gaseous D_2O over a Wide Range of Temperature and Pressure. J Phys Chem Ref Data 12: 933.
27. Reid RC, Prausnitz JM, Poling BE (1987) The Properties of Gases and Liquids, 4th (Edn.), McGraw-Hill0: pp: 656.
28. Atkins P, Paula J, Keeler J (2018) Atkins' Physical chemistry 11th (Edn.), Oxford University Press.
29. Kern CW, Karplus M (1972) The Water Molecule, Water-A Comprehensive Treatise 1: 37.
30. Easteal AJ, Woolf LA (1985) Pressure and temperature dependence of tracer diffusion coefficients of methanol, ethanol, acetonitrile, and formamide in water. J Phys Chem 89(7): 1066-1069.
31. Frohlich H (1949) Theory of Dielectrics: Dielectric Constant and Dielectric Loss, pp: 63.
32. F Booth (1951) The Dielectric Constant of Water and the Saturation Effect. J Chem Phys 19(4): 391.
33. Tarjus G, Kivelson D (1995) Breakdown of the Stokes–Einstein relation in supercooled liquids. J Chem Phys 103(8): 3071.
34. Jonas J, Defries T, Wilbur DJ (1976) Molecular motions in compressed liquid water. J Chem Phy 65(2): 582.